ACS OMEGA

http://pubs.acs.org/journal/acsodf

Article

Thermal Desorption Process Simulation and Effect Prediction of Oil-Based Cuttings

Xianyong Zhang,* Kai Li, and Aiguo Yao

Cite This: *ACS Omega* 2022, 7, 21675−21683

Read Online

ACCESS | Metrics & More | Article Recommendations

ABSTRACT: The disposal effect of thermal desorption of oil-based cuttings is predicted by analyzing the material temperature rise, heat transfer, and liquid evaporation in the processing. Based on the characteristics of material conveying in the heating bed, this paper establishes the governing equations for the simulation calculation of thermal desorption processing and demonstrates the correlation model between the mass change of wet components and the heat required. Changes in the material temperature and mass content of wet components in the process are calculated using the finite-volume method. The minimum temperature of the material layer experienced three stages: slow rising stage, stagnation stage, and rapid rising stage. In the first two stages, material preheating and water evaporation are the dominant processes. The third stage is mainly the evaporation of the oil phase. The inflection point between the second and third stages in the temperature rise curve can be regarded as the end point of water evaporation. During conveying, residence time and material layer thickness significantly influence the liquid phases removal ratio. The material drying area gradually expands from the boundary to the center with the extension of residence time, and the average mass fraction of liquids decreases slowly. The evaluation results from the final temperature and residual oil content of solid slag after disposal are consistent with the tests and have better accuracy in predicting the disposal effect when the heating temperature is higher and the residence time is longer.

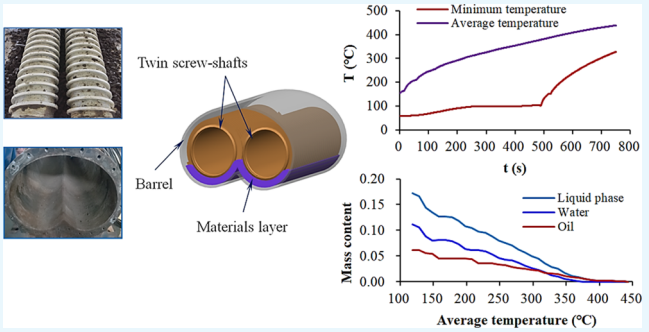

1. INTRODUCTION

Oil-based drilling cuttings, belonging to hazardous solid waste, are common industrial wastes of petroleum and natural gas exploitation. There are strict regulations on the disposal and discharge of oily cuttings in most countries, and these are becoming more and more stringent. Among various treatment methods of oil-based cuttings and oil-contaminated soil, thermal desorption is the one that has strong adaptability to material characteristics, high treatment efficiency, less secondary pollution, and convenient resource recovery, which have obvious advantages in industrial application.[1−4]

The reaction mechanism is different for different disposal temperature ranges. Thermogravimetric analysis is usually used to study the pyrolysis kinetics of oily sludge in a laboratory. The pyrolysis process of oil-field sludge mainly includes light organic vaporization, middle and heavy organic and carbonate decomposition, coke reduction, and other inorganic decomposition.[5] Modeling the pyrolyzed sample as a continuous mixture is feasible. Arrhenius-type kinetics was applied with activation energy, pre-exponential factor, and reaction order as continuous conversion functions.[6] Cheng et al. studied the pyrolysis behaviors of different oil sludge samples and compared them using the results of thermogravimetry (TG) and differential thermogravimetry (DTG) analysis. They also summarized the relationship between the DTG peak and surface properties of the oil sludge.[7] Ali et al. explored the thermal behavior of dried oily sludge pyrolysis by TGA and considered that heating rates significantly affected mass loss and peak temperatures.[8]

It was difficult to reflect the macro effect of heat and mass transfer characteristics in the material heating process due to the tiny mass of the sample. In the small-scale test, researchers mainly obtained thermal desorption effects under different experimental conditions. The effects of temperatures and treatment times on the thermal desorption efficiency were studied by the thermal desorption of oil-contaminated soils from a former landfill and gas station site in Korea.[9] The study showed that the different components of oil in the oil-contaminated soils could be treated effectively in a relatively short time by thermal desorption. Zhang et al. focused on the

Received: March 16, 2022
Accepted: June 3, 2022
Published: June 14, 2022

https://doi.org/10.1021/acsomega.2c01597
ACS Omega 2022, 7, 21675−21683

influence of heating temperature and residence time on the disposal effect. Thermal desorption of oily drilling cuttings was tested on the developed medium-sized experimental system, which adopted electromagnetic induction heating during the continuous conveying of materials by double screws.[10] Kang et al. studied the remediation of crude oil contaminated soil by continuous thermal treatment and found that temperature influenced the remediation efficiency more than the residence time.[11] Avsar et al. studied vacuum-assisted thermal drying of sludge, and results showed that the contribution on sludge drying of vacuum condition is more effective in drying time, especially at high temperatures.[12] Zhao et al. analyzed the flow patterns and physical parameters in the pyrolysis process of oil-based drilling cuttings and carried out numerical simulations of forced convection heat transfer inside a screw-driving spiral heat exchanger.[13] Microwave thermal desorption is a new method that has been recognized as a feasible technology for sludge disposal.[14,15] Guo et al. explored microwave drying behavior, specific energy consumption, average drying rate, energy efficiency, and drying effect. The results showed that the output power had the largest influence on specific energy consumption, energy efficiency, and drying efficiency, followed by the constant temperature and initial mass.[16] However, the current microwave drying systems exhibited high energy expenditures.[17] Most of these conclusions were based on experimental results, which were different due to different sludge characteristics and experimental conditions. The disposal efficiency strongly depends on the operational conditions of the process.[18]

The disposal equipment suitable for industrial application needs a continuous and efficient process. Screw reactors may become an attractive alternative technology for sewage sludge conversion, recovery, and recycling. The reactor combines the continuous conveying and heating of the material in a closed space to produce solid slag and vapors.[19] Mechanical compression is helpful to decrease the interfacial thermal resistance. The increase in mechanical load and the decrease in thickness improved the drying rates compared to those in the conventional drying process without a mechanical load.[20] During continuous operation, the energy consumption and disposal effect of continuous thermal desorption are closely related to material conveying characteristics, component content changes, and interphase heat and mass transfer during the process of oxygen isolation heating. There is a strong coupling of heat and mass transfer in the thermal desorption process, which has complex influencing factors. In thermal desorption, thermophysical parameters of oily sludge change dynamically with the increase in temperature and the phase change of wet components.[21] Liu et al. developed a kinetics model to study petroleum hydrocarbon desorption and analyzed the treatment cost using the established energy consumption model. It was found that the addition of sand to drill cuttings could increase the desorption rate.[22] The modeling and numerical simulation of drying in porous media were discussed by revisiting the different models of moisture migration during the drying process of porous media as well as their restrictions and applications.[23] Among the models and theories, mass and heat transport, and phase change (evaporation) were taken into account. The law of temperature increase during the in situ thermal remediation of the soil was experimentally studied.[24] The results showed that the soil temperature changes in three stages: concentrated heating section (the temperature increased from the ambient temperature to the boiling point of water), evaporation section (the water evaporated and the temperature maintained at the boiling point), and superheat section (the soil temperature continued to increase).

The thermal desorption mainly includes water and organic vaporization, and a small amount of thermal decomposition reaction. The main process in the heating unit is the liquid migration and phase change, which is dominated by physical changes.[25] Previous research studies on the thermal treatment of oil-contaminated soil or sludge were based on specific experimental conditions, and some effects of process conditions were studied. On this basis, through quantitative analysis under experimental conditions, the relevant dynamic characteristics were obtained. However, for the main process of liquid removal in thermal desorption, the discussion of heat and mass transfer characteristics was insufficient, and previous conclusions have inconveniences in engineering applications. Combined with a customized twin screw-shaft heating and conveying device, this paper simulated the thermal desorption process, and the treatment effect is predicted by analyzing the heating characteristics, heat transfer, liquid evaporation, and energy distribution.

2. MATERIAL CONVEYING AND HEATING CHARACTERISTICS

2.1. Conveying Device. The continuous transportation of materials under a heating state is the basis of the equipment's continuous operation. For thin-layer material conveying, the screw conveying shaft is specially designed, which has the characteristics of low speed, short pitch, and shallow groove. The adhesion characteristics of the material change significantly with a vast temperature increase. The material may stick to the wall and agglomerate in the process of thermal desorption. Therefore, conveying is designed as twin screw shafts, as shown in Figure 1. The customized design can self-clean the blade groove by meshing during rotation; on the other hand, it can also increase the heat transfer area.

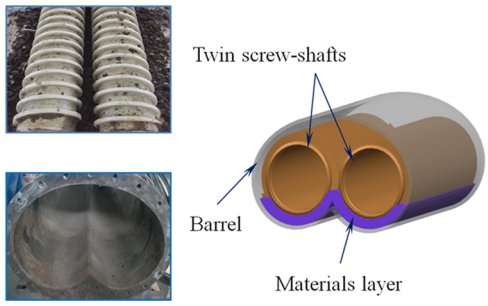

Figure 1. Twin screw shafts.

Figure 2 shows the geometric parameters of a screw shaft. The conveying capacity (Q) and the conveying residence time (t) are expressed as follows

$$Q(t) = zn_r\rho(t)\frac{\pi D_m}{\cos\beta}(S\cos\beta - e)h\varphi \quad (1)$$

$$t = \frac{60l}{n_r S} \quad (2)$$

where n_r is the rotating speed of the screw shaft, $\rho(t)$ is the material density at a particular time, z is the number of screw

https://doi.org/10.1021/acsomega.2c01597
ACS Omega 2022, 7, 21675−21683

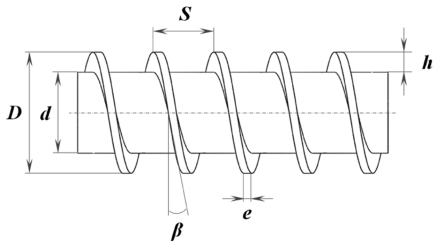

Figure 2. Geometric parameters of a screw shaft.

shafts, D_m is the middle diameter of the screw blade, β is the screw angle, S is the pitch of screw blade, e is the thickness of the blade, h is the depth of the spiral blade, φ is the filling factor of material volume, and l is the length of the screw shaft.

2.2. Conveying and Heating Characteristics. Liquid phases of oil-based cuttings are mainly water and mineral oil. Mineral oils are primarily the base oil added during the configuration of oil-based drilling fluid and the crude oil that may come from the formation during drilling. The oil-based cuttings generally require dewatering pretreatment before thermal desorption. The reduction of the sludge volume by decreasing most of the contained water saves the costs of transportation and further handling.[26] After the pretreatment, the total liquid content of oil-based cuttings is usually small (mass fraction is less than about 30%).

Screw shafts are set with a very low speed (about 2rpm) to prolong the residence time of processing. The mixing effect is not perceptible in the process of material conveying, which is mainly axial displacement.

The heating bed has two hot walls: one is the outer wall of the screw shaft and the other is the inner wall of the barrel. Both sides of the material layer are heated simultaneously in the thickness direction. The electromagnetic induction heating method is adopted, and the induction coil is wound on the outside of the barrel and the screw shaft's inner hole. The wall temperature generally exceeds the final distillation point of oil-bearing components. Under constant wall temperature, the surface temperature of the materials increases rapidly, wet components of the surface layer vaporize first, and the surface material begins to form a drying layer. As the temperature transfers to the inside, wet components gradually evaporate from the surface to the interior, and the drying layer extends to the inside until all layers have dried thoroughly.

After the vaporization of the liquid phases, the escape path of vapors is very short because the groove of the screw blade is designed to be shallow, and the material layer is thin. On the other hand, the vapors are quickly pumped away. The suction equipment can ensure that the system is in a micro negative pressure state, and the residence time of vapors in the device can be ignored.

3. CALCULATION MODELS

The volume shape of materials during screw conveying is shown in Figure 3. When screw shafts run at a very low speed, the volume shape of materials remains roughly unchanged during the conveying. Heat and mass transfers change in the x- and z-directions of the material and are uniform in the width direction (y).

3.1. Heat and Mass Transfer Equations. According to Fourier's law, the differential equation of material heat conduction is shown as follows

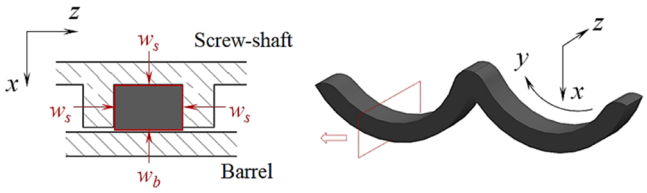

Figure 3. Volume shape of materials during conveying (one pitch of the screw blade).

$$\rho c\frac{\partial T}{\partial \tau} = \lambda\frac{\partial^2 T}{\partial x^2} + \lambda\frac{\partial^2 T}{\partial z^2} + q_v \tag{3}$$

The source term (q_v) in eq 3 is the heat flux caused by the phase change of wet components, which can be expressed as follows

$$q_v = -\frac{1}{V}\sum\left(h_{cj}\frac{\partial m_{cj}}{\partial t}\right) \tag{4}$$

where V is the volume of the control body, h_{cj} is the heat caused by each wet component phase change, and $\partial m_{c_j}/\partial t$ is the mass change rate of each wet component.

Start timing after the material enters the feeding port, the material heating residence time is equal to the material conveying residence time, which can be expressed as eq 2.

3.2. Equation Discretization. The finite-volume method is used to discretize the solution domain. In this method, the material stored in one pitch is taken as the micro control volume, as shown in Figure 3. Discrete variables in x- and z-directions are represented by subscripts i and k, respectively. The time step is Δt and is represented by the superscript n.

Diffusion term, unsteady term, and source term are expressed as follows

$$\begin{aligned}\Phi_\Gamma{}^{n+1} = {} & \lambda^n_{(i,k)}(y_i\Delta z)\frac{T^n_{(i+1,k)} - T^n_{(i,k)}}{\Delta x} + \lambda^n_{(i,k)}(y_i\Delta z)\\ & \frac{T^n_{(i-1,k)} - T^n_{(i,k)}}{\Delta x} + \lambda^n_{(i,k)}(y_i\Delta x)\frac{T^n_{(i,k-1)} - T^n_{(i,k)}}{\Delta z}\\ & + \lambda^n_{(i,k)}(y_i\Delta x)\frac{T^n_{(i,k+1)} - T^n_{(i,k)}}{\Delta z}\end{aligned} \tag{5}$$

$$\Phi_t{}^{n+1} = \rho^n_{(i,k)}c^n_{(i,k)}V_{(i,k)}\frac{T^{n+1}_{(i,k)} - T^n_{(i,k)}}{\Delta t} \tag{6}$$

$$\Phi_v{}^{n+1} = (q_v)^n_{(i,k)}V_{(i,k)} \tag{7}$$

The discrete equation of heat flow is expressed as follows

$$(q_v)^n_{(i,k)} = -\frac{1}{V_{(i,k)}}\sum_j\left(\frac{\Delta m^n_{cj(i,k)}h_{cj}}{\Delta t}\right) \tag{8}$$

Also, the conservation equation is shown as follows

$$\Phi_t{}^{n+1} = \Phi_\Gamma{}^{n+1} + \Phi_v{}^{n+1} \tag{9}$$

According to geometric parameters of the screw shaft, the y-direction dimension is related to the value of x and is expressed as follows

$$y_i = \pi(d + 2x_i)\varphi \tag{10}$$

In eq 8, $\Delta m^n_{cj(i,k)}$ is the mass change of each wet component in the control volume at a particular time. The supplementary

https://doi.org/10.1021/acsomega.2c01597
ACS Omega 2022, 7, 21675−21683

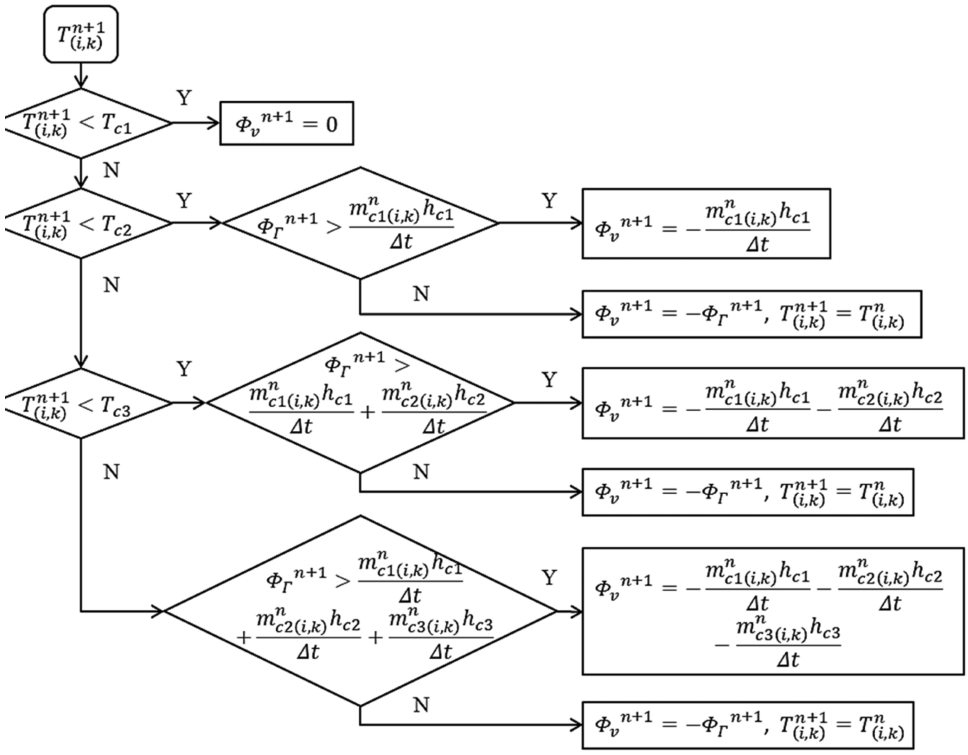

Figure 4. Energy distribution relationship of control volume during the increase in temperature.

relationship of these mass changes must be established to solve the equation.

3.3. Energy Distribution Mode. The factors affecting the mass change rate of wet components in the evaporation process are pretty complex. According to previous researchers' experimental research of sludge drying rate, the results are quite different due to the complexity of influencing factors and different experimental operating conditions. The usability of such results for the actual project is hard to satisfy. This paper discusses the mass change of each wet component from the requirements of energy matching and establishes the energy distribution mode. The supposed conditions are as follows:

(1) The fluidity of wet components in oil-based cuttings is not considered because their mass content is lower and generally in an unsaturated state.
(2) The residence time of vapors in the device is short after evaporation according to conveying and heating characteristics. The influence of steam diffusion on material temperature is not considered.
(3) There is no catalysis in the process of thermal desorption, and the maximum temperature is limited to 550 °C. The study does not consider a small amount of possible chemical reactions and only considers the evaporating process of each wet component.

In the process of the increase in material temperature in the control volume, when the temperature does not reach the initial boiling point (IBP) temperature of contained wet components, all of the heat transmitted to the control body is used to increase the material temperature. When the temperature reaches the IBP temperature of a wet component in the material, this wet component begins to evaporate. The evaporation sequence of wet components is arranged from low to high according to their IBP temperatures. The evaporation mass depends on the heat transferred into the control volume. If the heat transferred into the control body is still surplus after all wet components have evaporated, it continues to be used for increasing the material temperature. The wet components of oil-based drilling cuttings are mainly divided into three types (water, light oil, and heavy oil), and their IBP temperatures are set as T_{c1}, T_{c2}, and T_{c3}, respectively, and arranged in the order of $T_{c1} < T_{c2} < T_{c3}$. The energy distribution relationship of control volume during the increase in temperature is shown in Figure 4.

3.4. Boundary Conditions. The electromagnetic induction heating method is used to heat bed walls, and their temperatures are kept constant by controlling the heating controller. Contact surfaces between the heating bed and materials are isothermal boundaries that can be written as follows

$$\begin{cases} T|_{(x=0)} = T_{w_s} \\ T|_{(x=\delta_x)} = T_{w_b} \\ T|_{(z=0)} = T_{w_s} \\ T|_{(z=\delta_z)} = T_{w_s} \end{cases} \tag{11}$$

where T_{ws} and T_{wb} are the setting values of the temperature of the outer wall of the screw shaft and the temperature of the inner wall of the barrel, respectively; δ_x is the thickness of the material layer; and δ_z is the length of one pitch of the screw blade.

The initial condition is written as follows

$$T|_{(t=0)} = T_0 \tag{12}$$

where T_0 is the initial temperature, that is, the material temperature at the feed inlet of the heating bed.

3.5. Physical Property Parameters. The micro negative pressure is always maintained in the device during processing,

https://doi.org/10.1021/acsomega.2c01597
ACS Omega 2022, 7, 21675−21683

Table 1. Physical Property Parameters of Components (Condition of Atmospheric Pressure)

components	solid phase	liquid water	light oil	heavy oil
density/ρ(kg·m^{-3})	2300	1000	850	950
specific heat capacity/c(J·kg^{-1}·K^{-1})	840	4200	2600	2900
coefficient of heat conductivity/λ(W·m^{-1}·K^{-1})	0.45	0.68	0.14	0.12
latent heat of evaporation/h(J·kg^{-1})		2 258 000	250 000	190 000
temperature of initial boiling point/T_{IBP} (°C)		100	155	340
mass fraction/χ	82.7%	11.2%	5.5%	0.6%

which is close to the atmospheric pressure. The physical property parameters are taken under the condition of atmospheric pressure.

The average density of materials in the control volume at a particular time is expressed as follows

$$\rho^n_{(i,k)} = \alpha^n_{s(i,k)}\rho_s + \alpha^n_{c1(i,k)}\rho_{c1} + \alpha^n_{c2(i,k)}\rho_{c2} + \alpha^n_{c3(i,k)}\rho_{c3} \quad (13)$$

where ρ_s, ρ_{c1}, ρ_{c2}, and ρ_{c3} are the densities of the solid phase, liquid water, oil (I), and oil (II), respectively, and $\alpha^n_{s(i,k)}$, $\alpha^n_{c1(i,k)}$, $\alpha^n_{c2(i,k)}$, and $\alpha^n_{c3(i,k)}$ are the corresponding volume fractions material components in the control volume at a particular time.

The average specific heat capacity of materials in the control volume at a particular time is expressed as follows

$$c^n_{(i,k)} = \chi^n_{s(i,k)}c_s + \chi^n_{c1(i,k)}c_{c1} + \chi^n_{c2(i,k)}c_{c2} + \chi^n_{c3(i,k)}c_{c3} \quad (14)$$

where c_s, c_{c1}, c_{c2}, and c_{c3} are specific heat capacities of the solid phase, liquid water, oil (I), and oil (II), respectively, and $\chi^n_{s(i,k)}$, $\chi^n_{c1(i,k)}$, $\chi^n_{c2(i,k)}$, and $\chi^n_{c3(i,k)}$ are the corresponding mass fractions of material components in the control volume at a particular time.

In the process of thermal desorption, each component content of the materials changes with the increase in temperature. It is difficult to determine the dynamic variation characteristics of the thermal conductivity of the mixed materials because influencing factors are very complex.[27,28] The degree of saturation has a significant effect on thermal conductivity.[29] Based on Johansen's predictive model of the thermal conductivity of different types of soils,[30] the empirical formula of the average heat conductivity coefficient of mixed materials in the control volume is expressed as follows

$$\lambda^n_{(i,k)} = (\lambda_0 - \lambda_{dry})\left[1 + \lambda_{c1}\log\left(\frac{\alpha^n_{c1(i,k)}}{\alpha^0_{c1(i,k)}}\right) + \lambda_{c2}\log\left(\frac{\alpha^n_{c2(i,k)}}{\alpha^0_{c2(i,k)}}\right) + \lambda_{c3}\log\left(\frac{\alpha^n_{c3(i,k)}}{\alpha^0_{c3(i,k)}}\right)\right] + \lambda_{dry} \quad (15)$$

where λ_{c1}, λ_{c2}, and λ_{c3} are heat conductivity coefficients of liquid water, oil (I), and oil (II), respectively; $\alpha^n_{c1(i,k)}$, $\alpha^n_{c2(i,k)}$, and $\alpha^n_{c3(i,k)}$ are the corresponding volume fractions of liquid components in the control volume at a particular time; $\alpha^0_{c1(i,k)}$, $\alpha^0_{c2(i,k)}$, and $\alpha^0_{c3(i,k)}$ are the corresponding volume fractions of liquid components in the control volume at the initial time; and λ_0 and λ_{dry} are the heat conductivity coefficients of the materials in the initial state and a thoroughly dried state, respectively.

The physical property parameters of the contained components are shown in Table 1.

4. RESULTS AND DISCUSSION

4.1. Mesh Independence Checking. The finite-volume method is used to discretize the solution domain. The mesh independence has been considered by checking the temperature deviation in the calculation, as shown in Figure 5. The number of meshes in the cross section (XZ-plane) on the temperature deviation was investigated. The change in temperature deviation is obvious when the number of meshes is less than 350. When the number of meshes exceeds 350 and increases further, the result variation becomes gentle and stable.

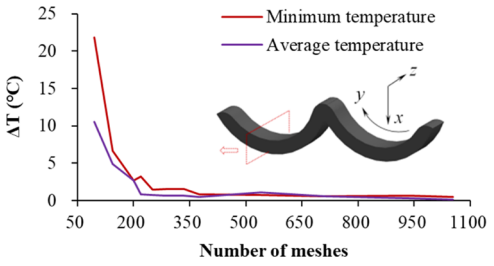

Figure 5. Change in temperature deviation with the number of meshes.

4.2. Temperature Changes. The wall temperature of the heating bed is set at 500 °C for the calculation. The material temperature distributions at different times are shown in Figure 6. It can be seen that the temperature gradually transfers from the boundary to the central area with the increase in residence time. The material temperature near the hot boundary increases rapidly due to the large temperature gradient near the hot wall. The lowest-temperature area is located at the center of the material layer, and this area gradually shrinks with the increase in residence time. After the low-temperature area shrinks to the center point, the temperature increases progressively.

The variations in materials' average temperature and minimum temperature are shown in Figure 7. The average temperature increases steadily with the extension of the residence time. The minimum temperature change of materials can be divided into three stages. The first is the slow rise stage (about 0−250 s) in which the temperature is less than 100 °C, which is the water evaporation temperature. The second is the sluggish stage (about 250−500 s) in which the minimum temperature of materials is almost unchanged. In this stage, the temperature reaches the water evaporation temperature but does not reach the oil phase IBP temperature, and thermal desorption is mainly water evaporation. The last stage is the rapid rise stage (more than 500 s). In this stage, the minimum temperature of materials increases rapidly, and the evaporation of oil phases is mainly completed. Figure 8 shows the lowest temperature (located in the center of the material layer) variation of different material thicknesses. In material conveying, the thinner the material layer is, the shorter the time required for temperature transfer to the center. When the material thickness increases, the duration of the first two stages

https://doi.org/10.1021/acsomega.2c01597
ACS Omega 2022, 7, 21675−21683

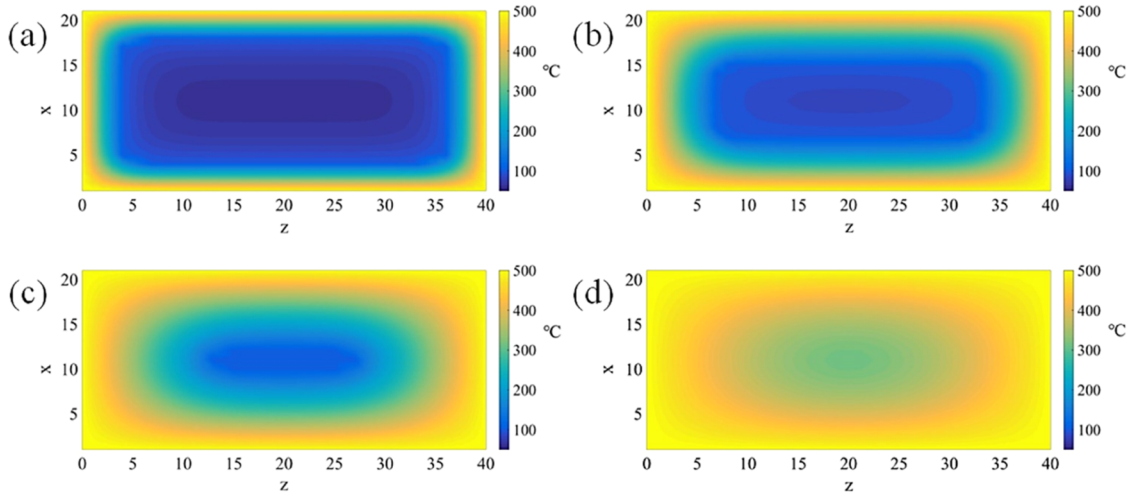

Figure 6. Material temperature distribution at different times: (a) 60 s, (b) 180 s, (c) 430 s, and (d) 750 s.

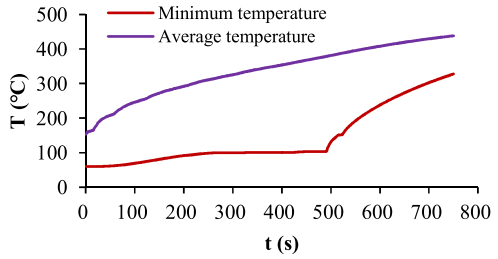

Figure 7. Material temperature variation.

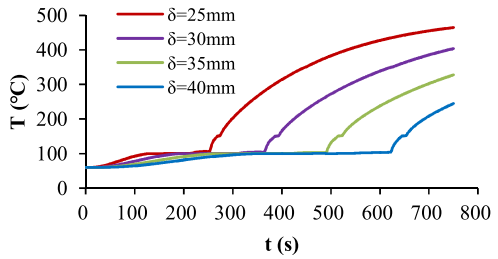

Figure 8. Lowest-temperature variation of different material thicknesses.

becomes longer. Therefore, the shallow groove design of the screw blade is necessary.

According to the minimum temperature variation characteristics of the material layer, it can be explained that material preheating and water evaporation are the dominant processes in the first two stages. The third stage mainly involves the evaporation of oil phases. In the temperature variation curve, the inflection point between the second and the third stage can be regarded as the end time of water evaporation. The heat required for water evaporation is much greater than that required for the oil phase due to the difference in their evaporation latent heats. Therefore, the water content of the material has a significant influence on the temperature rising. The water content of materials should be reduced as much as possible before thermal desorption to consider the efficiency and energy consumption. Some pretreatment methods, such as centrifugal dehydration, filter pressing, and low-temperature drying, can be used to reduce the initial water content of materials.

4.3. Mass Content Changes of Wet Components. With the extension of residence time, the material drying area gradually expands from the boundary to the center, as shown in Figure 9. After the material is conveyed to the heating bed

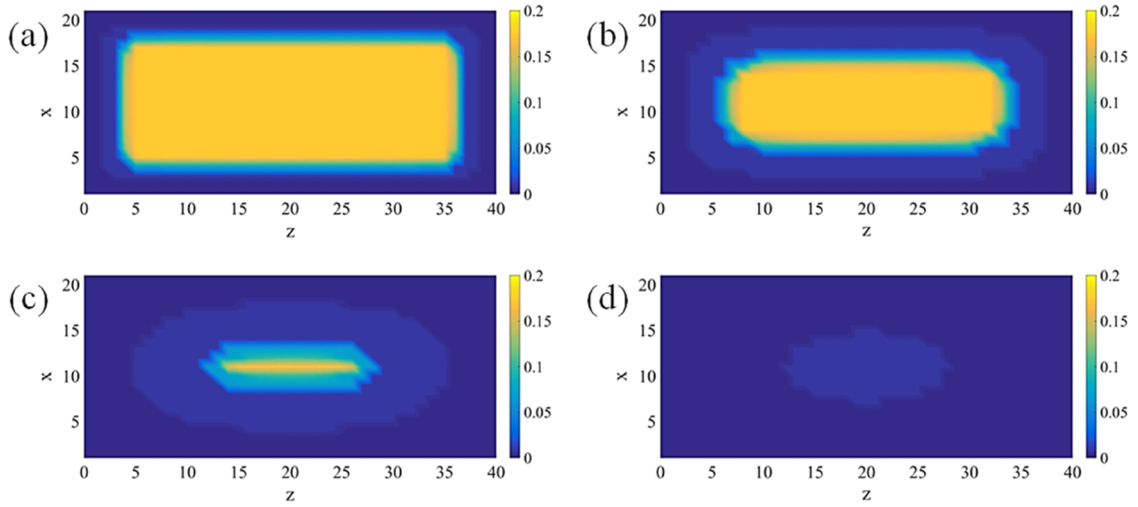

Figure 9. Mass fraction distribution of wet components at different times: (a) 60 s, (b) 180 s, (c) 430 s, and (d) 750 s.

https://doi.org/10.1021/acsomega.2c01597
ACS Omega 2022, 7, 21675−21683

from the feed inlet, wet components near the hot wall are removed in a relatively short time, and a drying zone begins to form. When the residence time reaches 430 s (discharge time corresponding to the screw-shaft speed of 3.5 rpm), there is still an area at the center that is not dry, and materials in this area still contain a certain proportion of liquid phases. When the residence time reaches 750 s (discharge time corresponding to the screw-shaft speed of 2.0 rpm), the drying area is fully extended to the central point, and all of the wet components are completely removed.

The average mass fraction changes in the solid phase and liquid with time are shown in Figure 10. The liquid mass

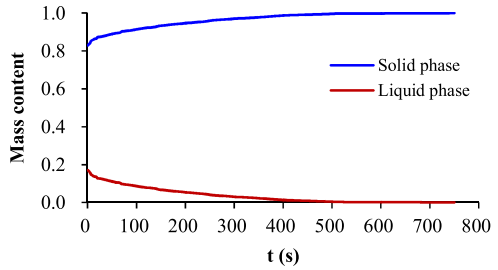

Figure 10. Average mass fraction changes of the solid phase and liquids.

fraction in the material decreases gradually with the increase in time. Figure 11 shows that when the time reaches about 500 s,

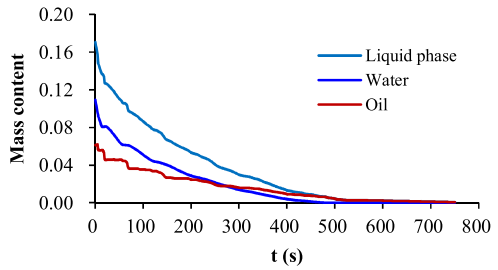

Figure 11. Average mass fraction changes of the contained water and oil.

the water is completely removed and the residual oil content is reduced to less than 1%. The residual oil decreases with the continuous increase in residence time, but the decrease rate gradually slows down. When the time reaches 750 s, the mass fraction of the residual oil is less than 0.1%, and the oil phase removal ratio is higher than 99%. Figure 12 shows the mass fraction variation of liquids with the average temperature change. With the increase in material's average temperature,

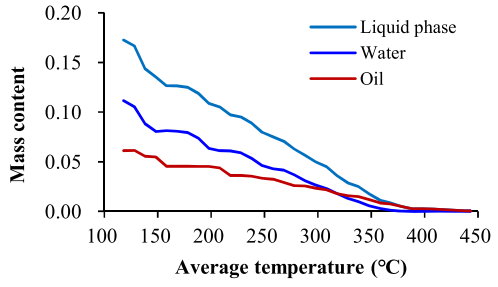

Figure 12. Variations in liquid mass fraction with the average temperature.

the water and oil contents decrease steadily. Compared with the oil content change, the water content decreases faster with the increase in the temperature. Most of the liquids are removed by enhanced evaporation when the average temperature reaches 350 °C, which is basically consistent with the volatilization temperature range of the liquids contained in oil-based drilling cuttings.

5. EXPERIMENTAL TEST

The sample of oil-based cuttings is taken from an oily sludge processing plant (Penglai, China). Its appearance is shown in Figure 13a and without flowability. The mass content of water

Figure 13. Oil-based cuttings (a) before and (b) after treatment.

is 11.2%, and the mass content of total petroleum hydrocarbons (TPHs) is 6.1%. In tests, the screw shaft runs at 3.5 and 2.0 rpm, and the corresponding residence times are 430 and 750 s. Test results and calculation results for different heating temperatures (from 350 to 550 °C) are compared.

The solid slag appearance is shown in Figure 13b. The temperature of the solid slag at the discharge port is measured, representing the highest temperature (final temperature) of the material during the thermal desorption process. Figure 14

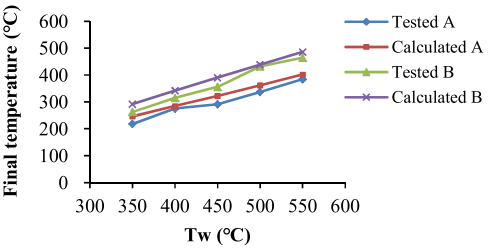

Figure 14. Comparison of final temperature.

shows the final temperature comparison of the solid slag. The test value of the discharge temperature is slightly lower than that calculated for different heating conditions. Figure 15 compares the TPH removal ratio after thermal desorption disposal. The difference between the calculated and experimental values decreases with the increase in heating

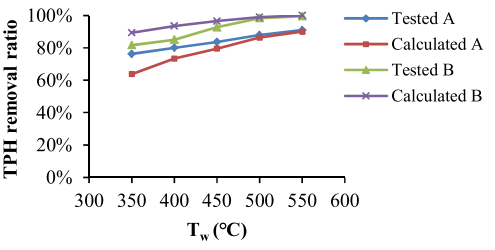

Figure 15. Comparison of TPH removal ratio.

https://doi.org/10.1021/acsomega.2c01597
ACS Omega 2022, 7, 21675−21683

temperature, which is less than 5% when the heating temperature reaches 500 °C or above.

From the comparison of results in Figures 13 and 14, it can be considered that the established calculation model is reasonable. This method accurately predicts the processing effect and is helpful in guiding the equipment design and further optimizing the treatment process.

6. CONCLUSIONS

The thermal desorption disposal effect is determined by characteristics of an increase in material temperature and changes in mass contents of wet components during processing. Based on the characteristics of material conveyed in the heating bed, governing equations of heat and mass transfer and energy distribution model in the processing are established and the thermal desorption disposal effect of oil-based cuttings can be predicted. Calculation results are relatively consistent with test results and better predict the disposal effect. This prediction method is based on energy balance, which has good robustness and could better meet the requirements of engineering calculation for equipment development and process parameter optimization.

In the process of thermal desorption, the minimum temperature characteristic of materials shows that the temperature changes in the first two stages (material preheating and water evaporation) are relatively slow and become rapidly after the water is completely removed. The initial water content of oil-based cuttings greatly influences the increase in temperature. For the harmless disposal of oil-based cuttings, we focus on the residual oil content. Therefore, the water content of initial materials should be reduced as much as possible because the treatment efficiency and energy consumption of industrial plants should be fully considered.

The residual oil content of the solid slag after thermal desorption can evaluate the disposal effect, which is closely related to the wall temperature of the heating bed and the conveying residence time. In general, the constant wall temperature of the heating bed can be controlled by the temperature control system. For industrial devices with continuous treatment, the heating residence time is determined by the material conveying time in the heating bed. The longer the residence time, the lower the residual oil content after treatment. However, too long residence time wastes energy because the continuous heating of the solid phase is no longer meaningful after wet components have been thoroughly removed. Therefore, the reasonable conveying residence time should be optimized when designing the heating bed device, which can be realized by comprehensively considering geometric parameters and the operating speed of screw shafts.

AUTHOR INFORMATION

Corresponding Author

Xianyong Zhang − *School of Mechanical Engineering, Yangtze University, Jingzhou 434023 Hubei, China;* orcid.org/0000-0002-3005-6182; Email: zhangxy@yangtzeu.edu.cn

Authors

Kai Li − *School of Mechanical Engineering, Yangtze University, Jingzhou 434023 Hubei, China*

Aiguo Yao − *Faculty of Engineering, China University of Geosciences, Wuhan 430074 Hubei, China*

Complete contact information is available at: https://pubs.acs.org/10.1021/acsomega.2c01597

Notes

The authors declare no competing financial interest.

ACKNOWLEDGMENTS

This work was supported by the Scientific Research Project of the Hubei Provincial Department of Education (D20211304). The authors would like to thank Chuanglian (Hubei, China) Petroleum Technology Co Ltd for experimental support.

REFERENCES

(1) Hu, G.; Liu, H.; Chen, C.; Hou, H.; Li, J.; Hewage, K.; Sadiq, R. Low-temperature thermal desorption and secure landfill for oil-based drill cuttings management: Pollution control, human health risk, and probabilistic cost assessment. *J. Hazard Mater.* **2021**, *410*, No. 124570.

(2) AlBeshr, K.; Al Hammadi, S.; Reddy, V. B.; Ali, E. A.; Mohammed, T. H.; Chauhan, D. K. Treatment of Legacy Oil Based Mud OBM Drill Cuttings and Sustainable Use of Recovered Materials, Paper presented at the Abu Dhabi International Petroleum Exhibition & Conference, SPE-183140-MS; Abu Dhabi, UAE, November 2016.

(3) Zhang, G.; Zhao, F.; Cheng, X.; Huang, S.; Zhang, C.; Zhou, M.; Mei, K.; Zhang, L. Resource utilization from solid waste originated from oil-based shale drilling cutting during shale gas development. *Chemosphere* **2022**, *298*, No. 134318.

(4) Zhao, C.; Dong, Y.; Feng, Y.; Li, Y.; Dong, Y. Thermal desorption for remediation of contaminated soil: A review. *Chemosphere* **2019**, *221*, 841−855.

(5) Miao, W.; Li, X.; Wang, Y.; Lv, Y. Pyrolysis characteristics of oilfield sludge and the comparison of kinetic analysis with two representative methods. *J. Pet. Sci. Eng.* **2019**, *182*, No. 106309.

(6) Wu, R. M.; Lee, D. J.; Chang, C. Y.; Shie, J. L. Fitting TGA data of oil sludge pyrolysis and oxidation by applying a model free approximation of the Arrhenius parameters. *J. Anal. Appl. Pyrolysis* **2006**, *76*, 132−137.

(7) Cheng, S.; Chang, F.; Zhang, F.; Huang, T.; Yoshikawa, K.; Zhang, H. Progress in thermal analysis studies on the pyrolysis process of oil sludge. *Thermochim. Acta* **2018**, *663*, 125−136.

(8) Ali, I.; Tariq, R.; Naqvi, S. R.; Khoja, A. H.; Mehran, M. T.; Naqvi, M.; Gao, N. Kinetic and thermodynamic analyses of dried oily sludge pyrolysis. *J. Energy Inst.* **2021**, *95*, 30−40.

(9) Choi, B.; Lee, S.; Jho, E. H. Removal of TPH, UCM, PAHs, and Alk-PAHs in oil-contaminated soil by thermal desorption. *Appl. Biol. Chem.* **2020**, *63*, No. 83.

(10) Zhang, X.; Yao, A. Pilot experiment of oily cuttings thermal desorption and heating characteristics study. *J. Pet. Explor. Prod. Technol.* **2019**, *9*, 1263−1270.

(11) Kang, C. U.; Kim, D. H.; Khan, M. A.; Kumar, R.; Ji, S. E.; Choi, K. W.; Paeng, K. J.; Park, S.; Jeon, B. H. Pyrolytic remediation of crude oil-contaminated soil. *Sci. Total. Environ.* **2020**, *713*, No. 136498.

(12) Avsar, Y.; Saral, A.; Ilhan, F.; Akyuz, B.; Gonullu, M. T. Vacuum-assisted thermal drying of wastewater treatment sludge. *J. Air Waste Manage.* **2021**, *71*, 293−303.

(13) Zhao, F.; Li, Y.; Liu, Z.; Tang, Y. Flow and heat transfer characteristics of oil-based drilling cuttings in a screw-driving spiral heat exchanger. *App. Therm. Eng.* **2020**, *181*, No. 115881.

(14) Hou, Y.; Qi, S.; You, H.; Huang, Z.; Niu, Q. The study on pyrolysis of oil-based drilling cuttings by microwave and electric heating. *J. Environ. Manage.* **2018**, *228*, 312−318.

(15) Alves, G. M.; Júnior, I. P. Microwave remediation of oil-contaminated drill cuttings − A review. *J. Pet. Sci. Eng.* **2021**, *207*, No. 109137.

(16) Guo, J.; Zheng, L.; Li, Z. Microwave drying behavior, energy consumption, and mathematical modeling of sewage sludge in a novel pilot-scale microwave drying system. *Sci. Total. Environ.* **2021**, *777*, No. 146109.

(17) Kocbek, E.; Garcia, H. A.; Hooijmans, C. M.; Mijatović, I.; Lah, B.; Brdjanovic, D. Microwave treatment of municipal sewage sludge: Evaluation of the drying performance and energy demand of a pilot-scale microwave drying system. *Sci. Total Environ.* **2020**, *742*, No. 140541.
(18) Bulmău, C.; Mărculescu, C.; Lu, S.; Qi, Z. Analysis of thermal processing applied to contaminated soil for organic pollutants removal. *J. Geochem. Explor.* **2014**, *147*, 298−305.
(19) Tomasi Morgano, M.; Leibold, H.; Richter, F.; Stapf, D.; Seifert, H. Screw pyrolysis technology for sewage sludge treatment. *Waste Manage.* **2018**, *73*, 487−495.
(20) Ma, D.; Ji, G.; Zhang, L.; Wang, D.; Liu, Q.; Ullah, F.; Li, A. Enhancement of conductive drying of sewage sludge with mechanical compression: Drying kinetics, and interfacial heat transfer behavior. *Sci. Total Environ.* **2021**, *796*, No. 148716.
(21) Layth, A. A.; Christelle, L.; Delphine, H.; Denise, B.; Marc, C. Thermal and mass transfer properties of a shrinkable industrial sludge: experimental determination and modeling approach. *Environ. Technol.* **2022**, *43*, 2230−2240.
(22) Liu, H.; Li, J.; Zhao, M.; Li, Y.; Chen, Y. Remediation of oil-based drill cuttings using low-temperature thermal desorption: Performance and kinetics modeling. *Chemosphere* **2019**, *235*, 1081−1088.
(23) Vu, H. T.; Tsotsas, E. Mass and heat transport models for analysis of the drying process in porous media: A review and numerical implementation. *Int. J. Chem. Eng.* **2018**, *2018*, No. 9456418.
(24) Wang, W.; Chen, C.; Xu, W.; Li, C.; Li, Y. Z. Experimental research on heat transfer characteristics and temperature rise law of in situ thermal remediation of soil. *J. Therm. Anal. Calorim.* **2022**, *147*, 3365−3378.
(25) Wang, B.; Wu, A.; Li, X.; Ji, L.; Sun, C.; Shen, Z.; Chen, T.; Chi, Z. Progress in fundamental research on thermal desorption remediation of organic compound-contaminated soil. *Waste Disposal Sustainable Energy* **2021**, *3*, 83−95.
(26) Elbaz, A. A.; Aboulfotoh, A.; ElGohary, E. H.; Reham, M. T. Review classification of sludge drying beds SDB (conventional sand drying beds CSDB, wedge-wire, solar, and vacuum assisted and paved drying beds PDB). *J. Mater. Environ. Sci.* **2020**, *11*, 593−608.
(27) Zhang, W.; Bai, R.; Xu, X.; Liu, W. An evaluation of soil thermal conductivity models based on the porosity and degree of saturation and a proposal of a new improved model. *Int. Commun. Heat Mass Transfer* **2021**, *129*, No. 105738.
(28) Ren, J.; Men, L.; Zhang, W.; Yang, J. A new empirical model for the estimation of soil thermal conductivity. *Environ. Earth Sci.* **2019**, *78*, No. 361.
(29) Alrtimi, A.; Rouainia, M.; Haigh, S. Thermal conductivity of a sandy soil. *Appl. Therm. Eng.* **2016**, *106*, 551−560.
(30) Zhang, N.; Wang, Z. Review of soil thermal conductivity and predictive models. *Int. J. Therm. Sci.* **2017**, *117*, 172−183.

https://doi.org/10.1021/acsomega.2c01597
ACS Omega 2022, 7, 21675−21683